JOURNAL OF THERMOPHYSICS AND HEAT TRANSFER
Vol. 8, No. 3, July–Sept. 1994

Monte Carlo Simulation of Radiating Re-Entry Flows

Jeff C. Taylor*
North Carolina State University, Raleigh, North Carolina 27695
Ann B. Carlson†
NASA Langley Research Center, Hampton, Virginia 23681
and
H. A. Hassan‡
North Carolina State University, Raleigh, North Carolina 27695

The direct simulation Monte Carlo method is applied to a radiating, hypersonic, axisymmetric flow over a blunt body in the near continuum regime. The ability of the method to predict the flowfield radiation and the radiative heating is investigated for flow over the Project Fire II configuration at 11.36 km/s at an altitude of 76.42 km. Two methods that differ in the manner in which they treat ionization and estimate electronic excitation are employed. The calculated results are presented and compared with both experimental data and solutions where radiation effects were not included. Differences in the results are discussed. Both methods ignore self absorption and, as a result, overpredict measured radiative heating.

Nomenclature

A = transition probability
g = degeneracy
h = Planck's constant, J s
K = excitation rate coefficient
M = third body
n = number density, part/m^3
Q = surface heat flux, W/cm^2
R = radius of the vehicle, m
S = distance along the surface, m
T = temperature, K
U = velocity, km/s
X = mole fraction
x, r, θ = axisymmetric coordinates, m or rad
ε = energy of a particle or state, J
η = distance normal to the surface, m
λ = wavelength, or mean free path, μ or m
ν = frequency, s^{-1}
ρ = density, kg/m^3
τ = relaxation time, s

Subscripts

c = convective value
e = value for electrons
el = value for electronic modes
eq = equilibrium value
j, k = values for state j, k
M = value for type M particles
R = radiative value
r = rotational value
stag = stagnation point value
t = translational value
v = vibrational value
w = wall value
∞ = freestream value

Superscript

$-$ = average quantity

Presented as Paper 93-2809 at the AIAA 28th Thermophysics Conference, Orlando, FL, July 6–9, 1993; received Aug. 12, 1993; revision received Dec. 6, 1993; accepted for publication Dec. 7, 1993.

*Research Assistant, Mechanical and Aerospace Engineering Department, Box 7910. Student Member AIAA.
†Research Scientist, Aerothermodynamics Branch, Space Systems Division, M/S 366. Senior Member AIAA.
‡Professor, Mechanical and Aerospace Engineering Department, Box 7910. Associate Fellow AIAA.

Introduction

THE current interest in re-entry and aerobraking vehicles requires an ability to calculate rarefied, hypersonic flows with high degrees of thermal and chemical nonequilibrium. The direct simulation Monte Carlo (DSMC) method of Bird[1] has proven to be an effective tool in calculating these types of flows. For many of these flows, the radiation from the shock layer can be a significant portion of the overall heating. Because of this, increased attention has been given to extending the method to treat flows with ionization and radiation.[2–9] The ability to calculate such flows may be necessary to effectively design the thermal protection systems required by these future vehicles.

Problems arise in the calculation of nonequilibrium radiation because of the large number of radiative states that exist, and because a significant amount of radiation can come from sparsely populated states and minor species. This requires a large number of simulated particles to avoid unacceptably large statistical scatter. To address these problems, Bird[4] proposed a radiation model which uses a phenomenological approach. Although Bird demonstrated the ability of the DSMC method to calculate flows with radiation, much of the data employed was somewhat approximate. Recently, Carlson et al.[6–8] have examined the ionization modeling and calculation of the electronic excitation numbers with the aim of improving the modeling of the physical processes present.

Due to the computational costs in simulating flows with ionization and radiation with the DSMC method, many previous works[2–8] have limited their computations to one-dimensional calculations. Such calculations did not address the effect of the plasma sheath on the surface properties. Furthermore, previous calculations[5] showed that using a one-dimensional stagnation streamline DSMC approach to predict the radiative heating would be deficient. Thus, the extension to two-dimensional/axisymmetric calculations is necessary to

examine radiative heating predictions. The ionization model developed in Refs. 6–8 was extended to two-dimensional/axisymmetric DSMC calculations by Taylor et al.[9] The proper calculation of surface properties necessitated the development of a sheath model. The goal of this work is to extend this two-dimensional/axisymmetric procedure to include both ionization and radiation, and to examine their effects on surface properties.

In order to determine the ability of the DSMC procedure to predict surface properties in an ionizing and radiating flow, calculations are conducted for the axisymmetric flow over the Project Fire II vehicle at 1634 s into the mission.[10] This point was in the near continuum region with an altitude and free-stream velocity of 76.42 km and 11.36 km/s, respectively. This case was chosen because some radiative heating was measured, but the conditions were such that the computational time for the DSMC calculations were still manageable. Differences between the modeling procedures are evaluated, and wherever possible, the results are compared with experimental measurements.

DSMC Method

The DSMC method, developed by Bird,[1–4] employs statistical methods to simultaneously calculate the trajectories of thousands of simulated particles. While these particles move through the domain, they interact with each other and with various boundaries. The position, velocity, and internal states of the various particles are stored and modified when interactions occur. The macroscopic flow properties are, in turn, calculated by averaging the local particle properties when a sufficiently large sample has been obtained. The surface properties are determined directly from the momentum and energy transfers between the simulated particles and the surface boundaries.

The physical models used in all of these calculations include the following. The variable hard sphere (VHS) model was used for the molecular interaction potential. The Larsen-Borgnakke model was used for the distribution of the energy to the different internal modes of the particles. Both of these models are the most widely used for the DSMC method and are detailed in Ref. 1. The modifications to the standard procedure include a model for temperature-dependent vibrational collision numbers, detailed in Ref. 11, and a local time stepping procedure described in Ref. 12. For the VHS model employed, the probabilities for the chemical reactions were selected in such a way to reproduce, at equilibrium, experimentally measured rate coefficients.[13] A total of 44 chemical reactions were used in the present study. The reaction rates were based on a set proposed by Park and Menees.[14] The coefficients for the first 41 reaction rates are tabulated in Ref. 6. The last three reactions are the recombination reactions for N_2, O_2, and NO. The rate coefficients for these reactions were obtained from curve fits of the equilibrium constants given in Ref. 15 and from the forward rates already obtained.

The addition of electrons to the flowfield through ionization requires some modification of the DSMC procedure. The electrons are characterized by extremely high velocities and collision frequencies compared to the other particles in the flow. This requires the DSMC calculations to use a very small computational time step, and this results in long computational times. Furthermore, because of the addition of charged particles in the flowfield, an electric field is created. This electric field which is created by the motion of the ions and electrons results in charged particle acceleration. This field is evaluated away from the sheath from ambipolar diffusion considerations. Furthermore, the plasma sheath that develops acts to insulate the surface from the electrons. More details on the modeling of the plasma sheath are presented in Appendix A. These and other issues relevant to the ionization process were dealt with in Refs. 6, 7, and 9. The models used to include radiation in the simulation will be outlined in more detail in the following section.

The Project Fire II surface was constructed of beryllium. Upon re-entry, the vehicle was exposed to the atmosphere, and BeO was believed to have formed. The catalytic recombination coefficient at the indicated surface temperature for BeO is thought[16] to have a value of about 0.02. This value was used for all DSMC calculations presented in this study.

Radiation Modeling

Consider the addition of nonequilibrium radiation modeling into the DSMC procedure. Although Bird has shown the ability of the DSMC method to calculated flows with radiation,[4] much of the data employed is somewhat approximate. In an attempt to remove some of the uncertainties and lead the modeling to a more accurate representation of the physical process present, Carlson and Hassan[8] have proposed some changes for the electronic excitation modeling. The calculations presented in this study will compare the two modeling procedures. Thus, a brief outline of the two procedures follows. A complete description of the radiation modeling is presented in Refs. 4 and 8.

First, consider the radiation modeling proposed by Bird.[4] The method includes electronic excitation and thermal radiation from bound-bound transitions only, which is known to be significant in flows on the order of 10 km/s. Because the number of radiative states is so large, and because a significant amount of radiation can come from minor species and sparsely populated states, the radiation modeling is calculated using a phenomenological model. The model is similar to the Larsen-Borgnakke model currently used for the rotational and vibrational excitation with some minor changes. Instead of assigning each computational particle a certain state, as with rotation and vibration, each particle is assigned a distribution over all available electronic states up to the dissociation or ionization energy. The distribution is an equilibrium distribution appropriate to the effective temperature based on the sum of the relative translational energy and the electronic energy of the particles in the collision. This allows a reasonable amount of computational particles to be used without unacceptably large statistical scatter. Because each computational particle represents a large number of actual particles, this procedure also is physically reasonable.

As in the excitation of the rotational and vibrational modes, the excitation rates for the electronic modes must be determined. Because little data is available on the excitation cross sections of the species involved in real air, Bird adopted a primarily qualitative method to demonstrate the capability of the method. Bird argued that the electron-ion and electron-neutral elastic cross sections are on the order of 10^{-15} cm^2, and that the electron impact excitation cross sections are on the order of 10^{-16} cm^2. This suggests the fraction of collisions that leads to electronic excitation should be about 0.1. Bird further argued that because of the assumption of a distribution over all electronic states, instead of a single state, that this number should be further reduced. These numbers apply to electron and ion impact collisions. The numbers are further reduced by a factor of 10 for neutral impact collisions.

The molecular band system employed is the same as that by Park[17] and involves the electronic states of molecular oxygen, neutral and ionized molecular nitrogen, and nitric oxide. These are tabulated in Ref. 4 along with the mean time to spontaneous emission. A computational restriction requires that the computational time step in the collision routine be less than the minimum radiative lifetime.[4] Thus, when radiation is included in the calculations, the computational time step is small and long computational times result.

Because of the large number of electronic states present in the atomic species, the states have been combined to form a manageable number of groups.[4] The radiative transitions are also grouped and are referred to by a number rather than spectroscopic code. As a result of the grouping, each transition will generally involve only a fraction of the states in the upper groups. The electronic states, radiation transition groups,

and participating fractions are tabulated for both the atomic oxygen and nitrogen in Ref. 4.

The radiation model employed by Carlson and Hassan[8] is the same as above, with the exception of the method for determining the electronic excitation numbers. Because of the approximate nature Bird used in calculating the electronic excitation numbers, Carlson and Hassan proposed a different method of calculating these numbers based on existing data, in order to remove uncertainties in the procedure. A detailed description of the method is presented in Ref. 8. A brief description of their procedure is as follows.

The reactions responsible for the bound-bound radiation are

$$M + B_j \leftrightarrow M + B_k \tag{1}$$

$$B_k \leftrightarrow B_j + h\nu \tag{2}$$

where j and k denote electronic states and $h\nu$ is the radiation emitted. The largest rates in the above reactions are for charged particle collisions. However, for a slightly ionized flow, neutral particle collisions are also important. Thus, Carlson and Hassan calculate the production rate of particles in some electronic state, multiply by the electronic energy of that state, and sum over all possible states. Setting this to a Landau-Teller form for τ, gives

$$n\frac{\mathrm{d}\bar{\varepsilon}_{\mathrm{el}}}{\mathrm{d}t} = \frac{\mathrm{d}}{\mathrm{d}t}\left(\sum \varepsilon_j n_j\right) \equiv \frac{n(\bar{\varepsilon}_{\mathrm{eq}} - \bar{\varepsilon}_j)}{\tau} \tag{3}$$

where n and n_j are the number density and the number density of particles in some electronic state j, respectively, and $\bar{\varepsilon}_{\mathrm{el}}$, $\bar{\varepsilon}_j$, and $\bar{\varepsilon}_{\mathrm{eq}}$ are the average electronic energy, the average electronic energy in state j, and the average equilibrium electronic energy, respectively. An estimate of $1/\tau$ is then given to be

$$\frac{1}{\tau} \simeq \frac{\sum \varepsilon_j n_j [K_M(j) n_M + A(j)]}{\sum \varepsilon_j n_j} \tag{4}$$

where

$$K_M(j) = \sum_k K_M(j, k)$$
$$A(j) = \sum_k A(j, k) \tag{5}$$

Here, $A(j, k)$ and $K_M(j, k)$ are the transition probability and excitation rate coefficients, respectively. Thus, the fraction of collisions that lead to electronic excitation is just equal to $1/\tau\nu$, where ν is the collision frequency. Also, since this is for electronic excitation by electron impact, the collision frequency used is that for the electrons. But, since electrons are minor species in the flow, local cell quantities will have large amounts of statistical scatter. Thus, average values over the whole domain for the relaxation times and collision frequencies are calculated and used in the simulation. The rate coefficients above are available from the NEQAIR radiation code of Park,[18] except for those for molecular oxygen and the highest excited level of molecular nitrogen. These values were obtained from Slinker and Ali.[19]

The above applies for electronic excitation by electron and ion impact. The cross sections for the collisions of neutral heavy particles are smaller than those of electron collision by approximately the ratio of the two masses.[17] Thus, the fractions for electronic excitation are reduced by this amount for neutral particles.

Furthermore, if the relaxation numbers are calculated correctly, then it will not matter whether the energy is assigned to a specific state, as with rotation and vibration, or a distribution of states, as with the electronic modes. Since the radiation is determined by the electronic energy, then as long as the average electronic energy is computed correctly, the electronic energy of the system will remain the same, regardless of how the energy is distributed among the electronic states. This means that when a large sample is considered, the results should not depend on the manner in which the average electronic energy is assigned. Therefore, a further reduction in the electronic excitation collision numbers should not be required.

Before the results are presented and discussed, a summary of the major differences between the two modeling procedures is given as follows. Note, the references to "Bird's method" will correspond to using the ionization and electronic excitation modeling presented by Bird,[4] and similarly, "current method" will correspond to using the ionization and proposed electronic excitation modeling presented in Refs. 6–8. For the ionization modeling, the major difference is in how the electrons are treated. In Bird's method, the motion of the free electrons is constrained to that of the ion from which it originated. For the current method, the free electrons are allowed to move freely and are affected by an electric field which is calculated from ambipolar diffusion considerations. Also, the current method employs a model for the plasma sheath that develops on the surface,[9] which is not used nor required with Bird's method. For the electronic excitation, Bird's method employs relaxation constants which were finely tuned using the AVCO experiment.[4] The current method uses data obtained mostly from the NEQAIR program, which should make it applicable over a wide range of conditions.

Another difference in the two methods is the computational resources required. The addition of ionization modeling using Bird's method requires little additional memory and computational time. However, the addition of radiation using Bird's method requires much smaller computational time steps, typically less than the time required for spontaneous emission, resulting in longer computational times. Also, there is a substantial memory increase required to store the electronic levels for each simulated particle with Bird's method. All calculations presented using Bird's method simulated approximately 250,000 particles, whereas the current method calculations simulate around 750,000 particles. This increase in the number of simulated particles used for the current modeling procedure is due to the ionization modeling used.[9] To calculate the local electric field for the current method, a meaningful sample of charged particles is required. This typically requires more global particles than needed for Bird's method. Also, longer calculations are required to smooth the electric field before steady state is established. The further addition of radiation modeling using the current method has the same memory increase requirements as Bird's method. However, since the current method already uses a reduced computational time step for the electron interactions, the addition of the radiation modeling does not affect the computational time step because collision times based on the electron collision frequency are comparable to the times required for spontaneous emission. The end result is that the computational times and memory required to include ionization and radiation using Bird's method are generally smaller than those using the current modeling procedure. Note, for all calculations presented involving radiation using either method, self absorption was neglected.

Results and Discussion

Results are presented for the axisymmetric simulation of the Project Fire II configuration at 1634 s into the mission. The vehicle was at an altitude of 76.42 km with the freestream flow conditions given in Table 1. The computational grid, shown in Fig. 1, consists of 18,000 cells (30 × 600), and was used for all computations presented. The grid requirements of the DSMC method were met for all cases shown.

For the first set of calculations, radiation was not included, and the ionization and electronic excitation were computed using Bird's method.[4] Figure 2 shows the convective heat

Table 1 Flow conditions for the Project Fire II vehicle at 1634 s

Property	Value	Units
Altitude	76.42	km
U_∞	11.36	km/s
ρ_∞	3.50836×10^{-5}	kg/m^3
n_∞	7.294×10^{20}	part/m^3
T_∞	194.602	K
λ_∞	2.318×10^{-3}	m
T_w	615	K
Q_c[a]	172.0 ± 5%	W/cm^2
$Q_{R,\text{stag}}$	8.2 ± 20%	W/cm^2

[a] @ S = 0.03 m.

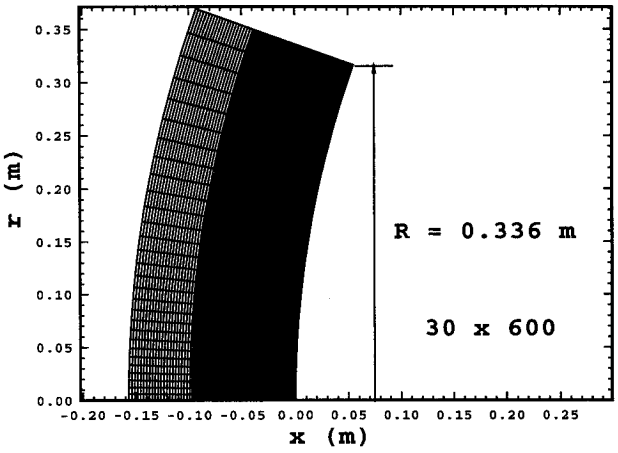

Fig. 1 DSMC computational grid used for Project Fire II calculations.

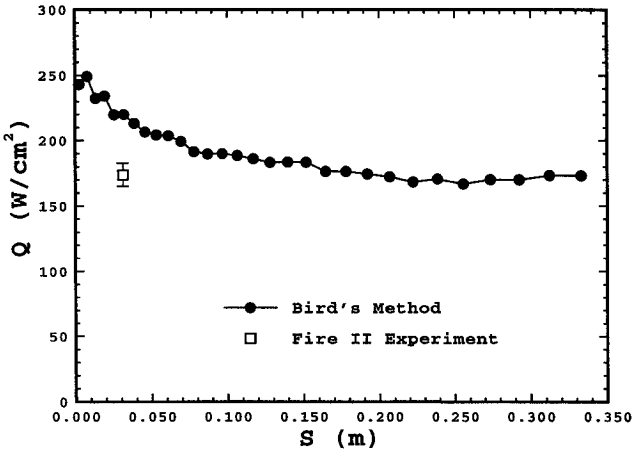

Fig. 2 Convective heat transfer along the surface for DSMC solution using Bird's method without radiation.

transfer Q_c as a function of distance along the surface of the vehicle S. Measured values[10] at S = 0.03 m yield a convective heating value of approximately 172 W/cm^2. The experimental error was given as ±5%. The variation along the surface for this case was not given, but similar experimental conditions showed a slight decrease in the heating as S increases. Present calculations yield a value of 220 W/cm^2 which decreased to 173 W/cm^2 at the shoulder. Thus, DSMC calculations overpredict the heat transfer in the stagnation region by 20–30%, but agreed much closer as S increased.

The distribution of the translational T_t, rotational T_r, vibrational T_v, and electron T_e temperatures along the stagnation line η are shown in Fig. 3. A high degree of nonequilibrium as well as a very high peak translational temperature are noted. This suggests that the inclusion of radiation may be important for any realistic simulation. Also, since the transfer of kinetic energy for collisions between heavy particles and electrons is very inefficient, the electron temperature does not equilibrate until very near the wall. Almost complete dissociation of both O_2 and N_2 was noted in the shock layer. In Fig. 4, the mole fractions of the electrons and major ions are shown along the stagnation line. The peak electron mole fraction occurs close to the body at a value of about 0.065. The major ion, N^+, also peaks at this point with a value of about 0.04. Note, directly after the shock, N_2^+ peaks at a value of about 0.018 and is locally the major ion present. Since N_2^+ is a strong radiator, this could be an important factor in the amount of radiation that would be predicted.

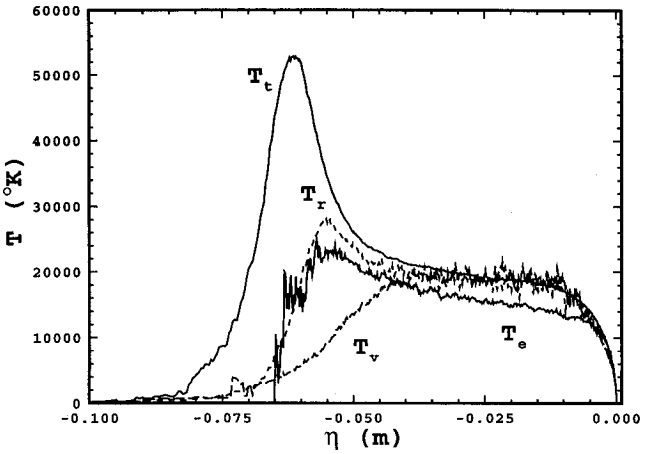

Fig. 3 Various temperatures along the stagnation line for DSMC solution using Bird's method without radiation.

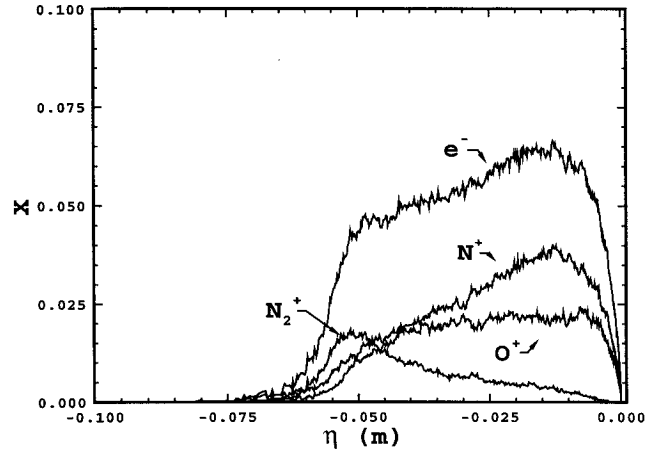

Fig. 4 Charged species mole fractions along the stagnation line for DSMC solution using Bird's method without radiation.

The next set of calculations include radiation and ionization using Bird's method in the DSMC simulation. Figure 5 shows a comparison of the convective heat transfer for the calculations with and without radiation with the Project Fire II experimental value. Very little change is noted with the inclusion of radiation. Thus, the DSMC calculations are still overpredicting the experimental values. Figure 6 shows a comparison of the radiative heat transfer from the total radiative spectrum and for part of the radiation spectrum. The partial radiation spectrum is the heat transfer calculated for radiation with wavelengths 0.2 μ and above. This is calculated to compare with the Project Fire II experimental values which were limited to this range from the measuring techniques employed.[20] The measured values[20] at the stagnation point for the radiative heat transfer yield a value of approximately 8.2 W/cm^2, with the experimental error given as ±20%. The present calculations show the predicted value at this location was 88.0 W/cm^2 for the heat transfer from radiation 0.2 μ and above, and was 202 W/cm^2 for the total radiative heating.

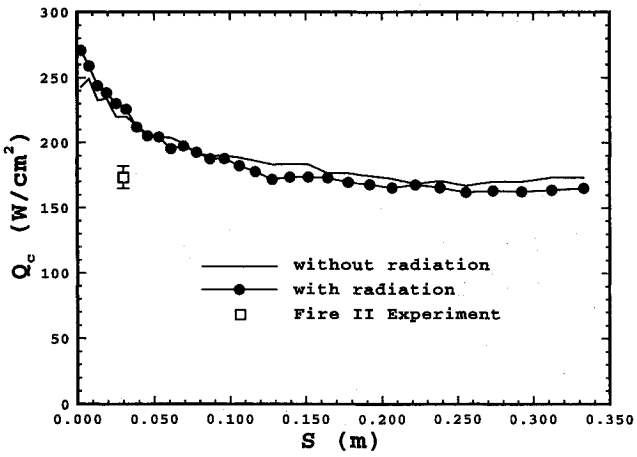

Fig. 5 Comparison of the convective heat transfer along the surface between DSMC solutions using Bird's method with and without radiation included.

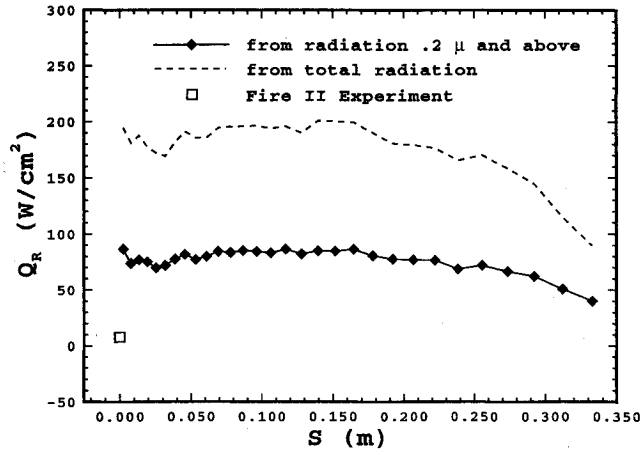

Fig. 6 Comparison of the radiative heat transfer along the surface for DSMC solution using Bird's method with Project Fire II experimental data.

Typically, almost all of the radiation less than 0.2 μ (uv radiation) will be self absorbed before reaching the surface, and will not contribute to the radiative heating.[21] Thus, the uv contributions can be neglected when approximating the amount of radiative heating which will realistically occur.

Previous calculations presented by Bird[4] showed excellent agreement in the surface radiative heating prediction for two Project Fire II cases. The calculations were conducted using a one-dimensional stagnation streamline DSMC code developed by Bird. It was noted later by Moss et al.[5] that predictions of the radiative surface heating using that one-dimensional stagnation line code would be deficient. While the radiative emission predicted would be correct, the surface radiative flux would not account for the radiation contribution to the surface from particles that were removed from the computational domain. The removal is a procedure required to simulate the stagnation line for these flows, and is described in Ref. 3. Thus, the radiative surface heating predictions using this code would be low. So, in light of this, the radiative heating predictions for the Project Fire II cases previously shown by Bird would also overpredict the measured radiative heating values.

A comparison of the distributions of the translational T_t and electron T_e temperatures along the stagnation line are shown in Fig. 7. The temperature shock occurs slightly later with the inclusion of radiation, but otherwise, little change is observed. Similar agreement is noted with the other flow properties and are not shown. The emission profiles for the molecular species and the separate atomic species are shown

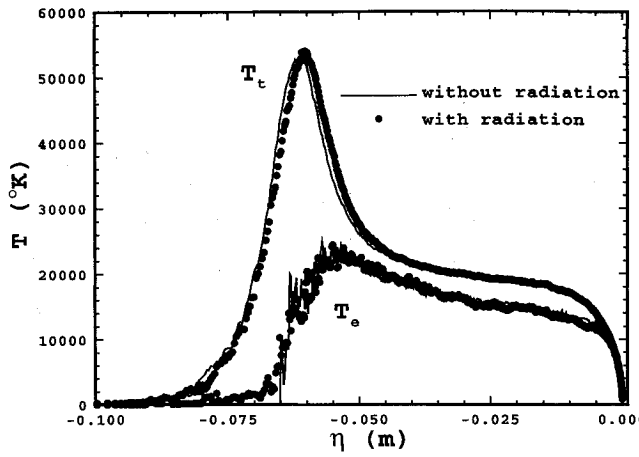

Fig. 7 Comparisons of the translational and electron temperatures along the stagnation line between DSMC solutions using Bird's method with and without radiation included.

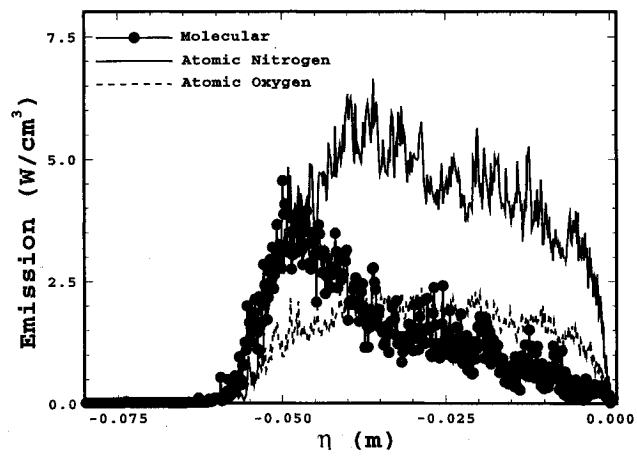

Fig. 8 Emission profiles along the stagnation line for DSMC solution using Bird's method.

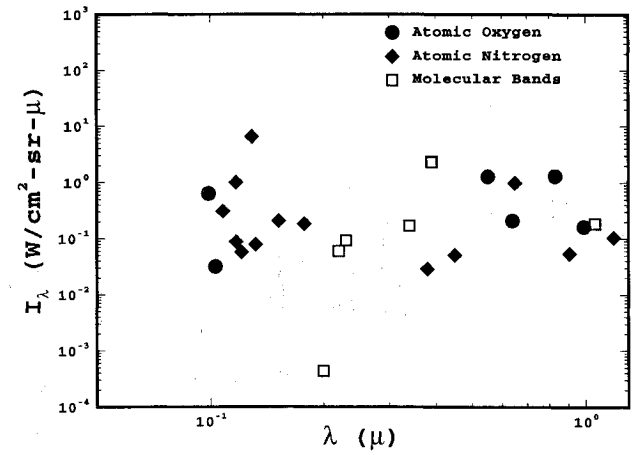

Fig. 9 Predicted radiation spectrum at the stagnation point for DSMC solution using Bird's method.

in Fig. 8. The atomic nitrogen is seen to be the major contributor for the emission throughout the shock layer, consisting of at least half of the emission at all points. It should also be noted that the molecular contribution consists almost solely of N_2^+ emission. The spectral intensities I_λ are shown at the stagnation point in Fig. 9. The major line responsible for most of the radiative heating is at 0.129 μ, which is the N,4 line from the atomic line grouping for N.[4] The next major contributor is the N_2^+ (1−) band system at 0.39 μ. Together,

these two are responsible for 54% of the radiative heating at the stagnation point for this case.

The last set of calculations are including radiation and ionization using the current modeling procedure described earlier. Figure 10 shows a comparison of the radiative heat transfer between the DSMC simulations using the two radiation modeling procedures with the experimental value. The new electronic excitation procedure calculates electronic collision numbers much less than the values presented by Bird. This was also seen in the one-dimensional calculation presented in Ref. 8. This results in a much faster excitation of the electronic levels of the species directly behind the shock. Thus, differences in the emission profiles and important radiation lines between the two methods are to be expected. As is seen from Fig. 10, the present model predicts a similar radiative flux when contributions from all wavelengths are considered, yet it yields a value close to the experimental measurements when only contributions from 0.2 μ and above are considered. Thus, the current method is predicting more uv radiation than Bird's method. Although radiation below 0.2 μ is expected to be absorbed, the present method cannot be declared superior to Bird's method. Such a conclusion has to await the incorporation of a model that accounts for absorption and bound-free transitions.

The translational temperatures T_t are compared between the two radiation models in Fig. 11. The profiles are still basically the same, yet the shock standoff distance and the equilibrium temperature have decreased. This is possibly the result of the considerable increase in the radiation from the

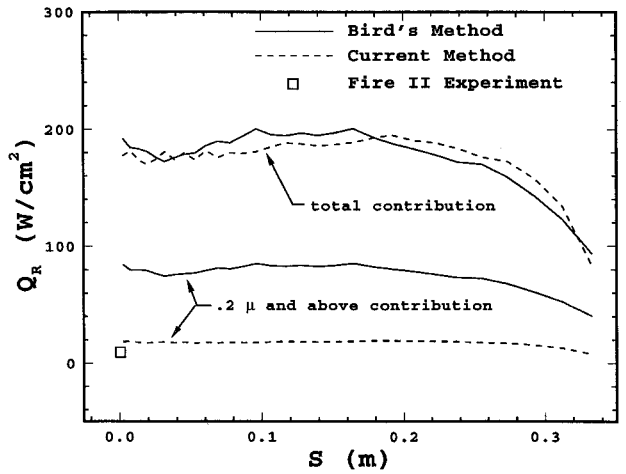

Fig. 10 Comparison of the radiative heat transfer along the surface between DSMC solutions using Bird's method and the current method.

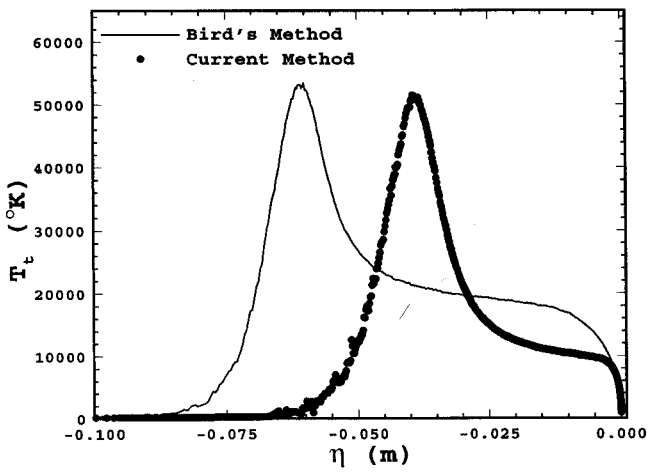

Fig. 11 Comparison of the translational temperatures along the stagnation line between DSMC solutions using Bird's method and the current method.

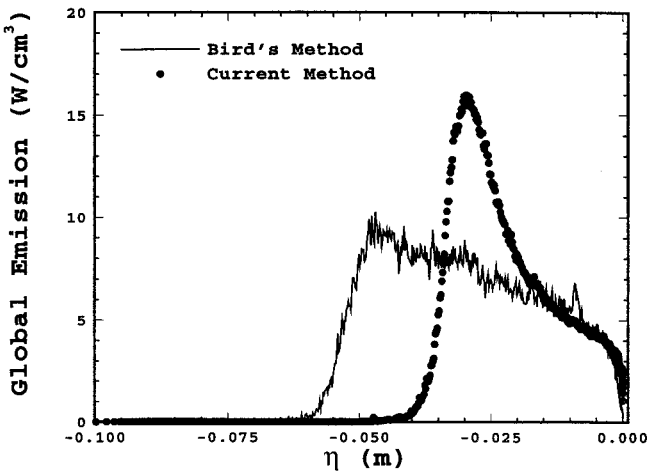

Fig. 12 Comparison of the global emission along the stagnation line between DSMC solutions using Bird's method and the current method.

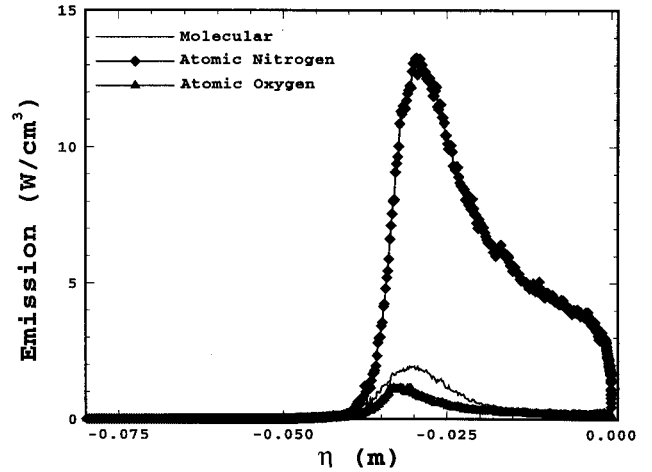

Fig. 13 Emission profiles along the stagnation line for DSMC solution using the current method.

uv spectrum. Since the uv radiation is not allowed to be reabsorbed, this results in substantial energy loss by the flow, and thus, the shock standoff distance decreases. Similar trends were noted for the other flowfield properties. A comparison of the global emission between the two methods is given in Fig. 12. Due to the faster excitation of the electronic levels, the global emission directly behind the shock is higher than that predicted by Bird's method. Also, the emission profiles for atomic oxygen and the molecular species using the new method, seen in Fig. 13, are very similar to profiles using Bird's method, seen in Fig. 8. Note, however, that the magnitudes are slightly different. Furthermore, the amount of emission from the atomic nitrogen predicted from the current method is nearly twice that predicted by Bird's method. Thus, the atomic lines and molecular band systems responsible for the majority of the radiation emission are quite different between the two methods.

Lastly, the spectral intensities at the stagnation point for the current method are given in Fig. 14 for the molecular bands, atomic nitrogen lines, and atomic oxygen lines. Comparing this figure to Fig. 9, the important point is that the current method shows nearly half an order of magnitude drop in the N_2^+ $(1-)$ band intensity. Whereas the molecular contribution dropped, the contribution from the atomic nitrogen lines increased by an order of magnitude for 2 or 3 of the uv radiation lines. Also, there is a noted drop in the intensity for the atomic oxygen lines in the IR radiation range. These figures show that the electronic relaxation numbers have a significant effect on the flowfield, and thus, on which radiative

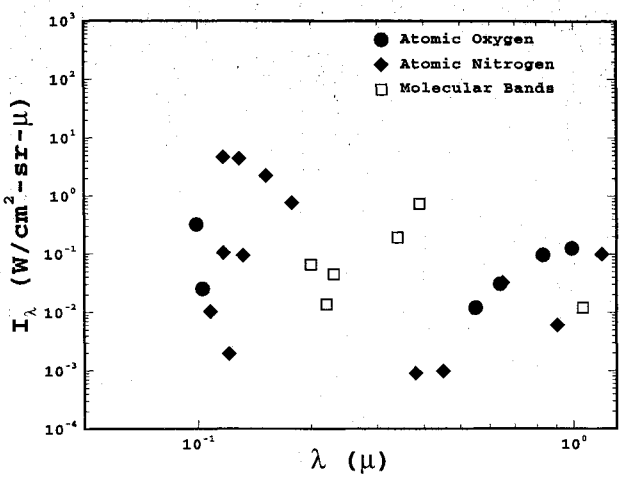

Fig. 14 Predicted radiation spectrum at the stagnation point for DSMC solution using the current method.

mechanisms become prominent. In turn, this significantly affects the radiative heating predictions.

Concluding Remarks

A new radiation modeling procedure proposed by Carlson and Hassan[8] has been extended to two-dimensional/axisymmetric DSMC calculations for weakly ionized, radiating, hypersonic flows. Using this method, the radiating, axisymmetric flow over the Project Fire II vehicle at 1634 s into the mission was investigated. Comparing results using the current method with those using the radiation model developed by Bird[4] showed that the electronic relaxation numbers can significantly alter the prominent radiative mechanisms and the amount of radiative heating calculated. Thus, accurate modeling of the electronic relaxation and calculation of the electronic excitation numbers is very important in correctly predicting radiation for these types of flows. Although the present model predicts radiative heating representative of the experiment when contributions are limited to wavelengths 0.2 μ and above, the result may be fortuitous. The current procedure needs to incorporate an absorption model before such a claim can be accepted.

Appendix: Modeling of Surface Plasma Sheath

When an ionized gas flows over a surface, an extremely large electric potential develops over a thin region between the plasma and the wall. The thickness of this region, called a plasma sheath, is on the order of the Debye length which is given by

$$d = \sqrt{\frac{kT_e}{4\pi n_e e^2}} = 6.90\sqrt{\frac{T_e}{n_e}}\ \text{cm} \qquad \text{(A1)}$$

where T_e is in Kelvin, and n_e is the number of electrons per cm^3. For the surface conditions presented, the local Debye length d, is much smaller than the local mean free path λ. Thus, intermolecular collisions within the sheath can be neglected, and particles are assumed to only interact with the sheath and the surface. This sheath affects the plasma by insulating the surface from the electrons, while accelerating the ions to the surface.[22] Also, since the surfaces modeled are considered to be electrically conducting, the surface will be fully catalytic to the ions. That is, ions will combine with available electrons to neutralize on contact with the wall, and thus, their ionization potential will be released to the wall.

Generally, in the DSMC method, all particles are assumed to reflect according to the classical diffuse model[23] with complete thermal accommodation to the surface temperature. Due to the plasma sheath, this model alone is not sufficient to model the surface reflections of the charged particles. Thus, a simplified model is introduced to account for the influence of the surface sheath on the charged particles.

First, consider the effects of the plasma sheath on the electrons. The potential barrier resulting from the presence of the sheath prevents most of the electrons from reaching the surface. As a result, only a very small fraction of the highly energetic electrons can penetrate the sheath. Also, since no intermolecular collisions are assumed to occur in the sheath, the velocity of the electrons exiting the sheath can be assumed to be directly related to the velocity entering the sheath. Assuming the local sheath potential varies only normal to the surface, then the velocity of the electrons exiting the sheath will have the same tangential component and the opposite normal component of the velocity entering the sheath. This behavior can be modeled by allowing the electrons to reflect specularly from the surface.[23] Thus, reflecting the electrons specularly results in no net electron energy flux to the surface.

Next, consider the acceleration of the ions to the surface as a result of the plasma sheath. This acceleration increases the amount of energy imparted to the surface by the ions. On average, the ions reach the surface with thermal energy $2kT_i$ plus the sheath potential energy $|e\phi|$.[22] In addition, the ions recombine with available electrons to release their ionization energy to the surface. The current modeling used for surface reflections is sufficient to model the thermal energy and the recombination energy contributions. But, for ion surface reflections, the sheath potential energy needs to be calculated and added.

To calculate the sheath potential ϕ, the procedure used by Camac and Kemp[22] is employed. Since the sheath potential adjusts to allow no net current to cross,[22] the sheath potential is calculated by setting the electron current towards the surface equal to the total positive current, i.e.

$$(n_e\bar{c}_e/4)\exp(-e\phi/kT_e) = (n_ic_i/4) + J \qquad \text{(A2)}$$

where n_i and n_e are the ion and electron number densities at the edge of the sheath, and $\bar{c}_e$ is the mean thermal velocity for the electrons, and J is the wall electron emission. Because of charge neutrality at the edge of the sheath, $n_i = n_e$. The term c_i is determined by the drift velocity of the ion in the sheath. Because intermolecular collisions are assumed negligible in the sheath, the value of c_i is given by[22]

$$c_i = 4\sqrt{(kT_e/m_i)} \qquad \text{(A3)}$$

In addition, J is assumed to be negligible. Also, $\bar{c}_e$ is given by[23]

$$\bar{c}_e = (2/\sqrt{\pi})\sqrt{(2kT_e/m_e)} \qquad \text{(A4)}$$

After substituting the above equations, the sheath potential reduces to

$$\phi = \frac{kT_e}{2e}\ln\left[\frac{1}{2\pi}\left(\frac{m_i}{m_e}\right)\right] \qquad \text{(A5)}$$

Thus, the sheath potential becomes only a function of T_e. Therefore, the modeling of the ion surface reflections involves calculating a local value of T_e, and then, obtaining the local sheath potential from Eq. (A5). After the ion diffusely reflects and recombines with an electron, releasing its ionization energy to the surface, the sheath potential energy $|e\phi|$ is added to the energy imparted to the surface to account for the sheath effects.

Acknowledgments

This work is supported in part by NASA's Cooperative Agreement NCCI-112 and the Mars Mission Center funded by NASA Grant NAGW-1331. The authors would like to

thank G. A. Bird for his guidance and advice. Also, the authors would like to acknowledge helpful discussions with Lin Hartung and Robert Greendyke.

References

[1]Bird, G. A., "Monte Carlo Simulation in an Engineering Context," *Rarefied Gas Dynamics*, edited by S. S. Fisher, Vol. 74, Pt. 1, Progress in Astronautics and Aeronautics, AIAA, New York, 1981, pp. 239–255.

[2]Bird, G. A., "Low Density Aerothermodynamics," AIAA Paper 85-0994, June 1985.

[3]Bird, G. A., "Direct Simulation of Typical AOTV Entry Flows," AIAA Paper 86-1310, June 1986.

[4]Bird, G. A., "Nonequilibrium Radiation During Reentry at 10 Km/sec," AIAA Paper 87-1547, June 1987.

[5]Moss, J. N., Bird, G. A., and Dogra, V. K., "Nonequilibrium Thermal Radiation for an Aeroassist Flight Experiment Vehicle," AIAA Paper 88-0081, Jan. 1988.

[6]Carlson, A. B., Hassan, H. A., and Moss, J. N., "Monte Carlo Simulation of Reentry Plasmas," AIAA Paper 89-0683, Jan. 1989.

[7]Carlson, A. B., and Hassan, H. A., "Direct Simulation of Reentry Flows with Ionization," *Journal of Thermophysics and Heat Transfer*, Vol. 6, No. 3, 1992, pp. 400–404.

[8]Carlson, A. B., and Hassan, H. A., "Radiation Modeling with Direct Simulation Monte Carlo," *Journal of Thermophysics and Heat Transfer*, Vol. 6, No. 4, 1992, pp. 631–636.

[9]Taylor, J. C., Carlson, A. B., and Hassan, H. A., "Monte Carlo Simulation of Reentry Flows with Ionization," AIAA Paper 92-0493, Jan. 1992.

[10]Cornette, E. S., "Forebody Temperatures and Calorimeter Heating Rates Measured During Project Fire II Reentry at 11.35 Kilometers Per Second," NASA TM X-1305, Nov. 1966.

[11]Olynick, D. P., Moss, J. N., and Hassan, H. A., "Grid Generation and Adaptation for the Direct Simulation Monte Carlo Method," *Journal of Thermophysics and Heat Transfer*, Vol. 3, No. 4, 1989, pp. 368–373.

[12]Olynick, D. P., Moss, J. N., and Hassan, H. A., "Monte Carlo Simulation of Re-Entry Flows Using a Bimodel Vibration Model," *Journal of Thermophysics and Heat Transfer*, Vol. 4, No. 3, 1990, pp. 273–277.

[13]Bird, G. A., "Direct Simulation of Multi-Dimensional and Chemically Reacting Flows," *Rarefied Gas Dynamics*, edited by R. Campargue, CEA, Paris, 1979, pp. 365–388.

[14]Park, C., and Menees, G. P., "Odd Nitrogen Production by Meteoroids," *Journal of Geophysical Research*, Vol. 83, Aug. 1978, pp. 4029–4035.

[15]Gupta, R. N., Yos, J. M., Thompson, R. A., and Lee, K. P., "A Review of Reaction Rates and Thermodynamic and Transport Properties for an 11-Species Air Model for Chemical and Thermal Nonequilibrium Calculations to 30000 K," NASA Reference Publication 1232, Aug. 1990.

[16]Clark, R. K., private communication, NASA Langley Research Center, Hampton, VA.

[17]Park, C., "Thermal Design of Aeroassisted Orbital Transfer Vehicles," Vol. 96, Progress in Astronautics and Aeronautics, AIAA, New York, 1985, pp. 395–418.

[18]Park, C., "Nonequilibrium Air Radiation (NEQAIR) Program: Users Manual," NASA TM 86707, July 1985.

[19]Slinker, S., and Ali, A. W., "Electron Excitation and Ionization Rate Coefficients for N_2, O_2, NO, N, and O," Naval Research Lab., NRL Memorandum Rept. 4756, 1982.

[20]Cauchon, D. L., "Radiative Heating Results from the FIRE II Flight Experiment at a Reentry Velocity of 11.4 Kilometers per Second," NASA TM X-1402, July 1967.

[21]Greendyke, R. B., and Hartung, L. C., "A Convective and Radiative Heat Transfer Analysis for the Fire II Forebody," AIAA Paper 93-3194, July 1993.

[22]Camac, M., and Kemp, N. H., "A Multitemperature Boundary Layer," Avco-Everett Research Lab., Research Rept. 184, Everett, MA, Aug. 1964.

[23]Bird, G. A., *Molecular Gas Dynamics*, Oxford Univ. Press, London, 1976.